より、RMSD（root mean square deviation:平均二乗偏差)、RMSF（root mean square fluctuation: 根平均二乗ゆらぎ)、およびDCCM（Dynamics Cross Correlated Motion:動的相互相関運動）を計算した。

（倫理面への配慮）

本研究では、特定の研究対象者は存在せず、倫理面への配慮は不要である。

## C．研究結果

分子動力学計算における構造変化を知るために初期構造からのRMSDを調べた。RMSDは約4nsまでに急激に増加し、その後約20nsまで緩やかに増加する。約20ns以上ではほぼ一定となり、平衡に達したと考えられる。

図１Aに分子動力学計算により得られた平衡構造を示す。平衡構造を見ると、V1/V2領域およびV3領域はN末端領域およびC末端領域から最も離れた位置にある。V1/V2領域は内側ドメインから外側ドメインに向かって配置され、V3領域は外側ドメインから内側ドメインに向かって配置されていた。V1/V2領域はV3領域の近傍に位置していた。この結果はM. Guttmanら(J. Virol, 86:8750-64,2012.)の小角X線散乱の溶液中での構造と一致する。

次に、HIV-1 gp120の大きくゆらぐ部位を知るためにRMSFを調べた。RMSFが大きい部位はいずれもループであり、V1/V2領域やV3領域のゆらぎが大きかった。また、内側ドメインと外側ドメインを比較すると、内側ドメインのバックグランドは外側ドメインのバックグランドよりも大きく、内側ドメインのゆらぎは外側ドメインよりも大きいことが示唆される。

HIV-1 gp120に見られるゆらぎの中で、相関運動する部位を知るために、DCCM解析を行った。図１BにDCCM解析により得られた分散共分散行列を示す。V1/V2領域にV3領域、N末端領域およびC末端領域との間に弱い正の相関運動が見られ、外側ドメインとの間に弱い負の相関運動が見られた。また、V1/V2 stemにβ20/β21ループとの間に正の相関運動が見られた。

HIV-1 gp120全長単量体分子モデルを、クライオ電子顕微鏡法により得られた既存の構造に重ね合わせることにより、HIV-1 gp120全長三量体分子モデルを構築した。（図２）V1/V2領域はウイルス粒子の最外殻に配置される。糖鎖がgp120外側ドメインおよびV1/V2領域にあるため、gp120はほぼ全体が糖鎖に覆われる。V3先端は三量体の中心に向かって配置され、抗体などのアクセスが制限される位置にある。

## D．考察

得られた構造が機能構造であるかどうかについて検討する。感染受容体であるCD4との結合後、動的性質から以下のような構造変化が誘起されると考えられる：(i) V1/V2 stemはβ20/β21ループとbridging sheetを形成するためにCD4近傍に移動する。(ii) V1/V2領域も大きく構造変化しV3領域近傍からCD4に近づく。(iii) DCCM解析より、V1/V2領域はN末端領域およびC末端領域との間に弱い正の相関運動、および外側ドメインとの間に弱い負の相関運動をするので、gp120三量体では外側ドメインが開くことになり、安定にCD4が結合できる。(iv) 最後に、V3領域が最外郭に配置され、コレセプタとの結合が可能となる。この一連の構造変化はM. Guttmanらの小角X線散乱の報告(J. Virol, 86:8750-64,2012.)やJ. Liuらのクライオ電子顕微鏡の報告（nature, 455:109-13, 2008.）と一致する。したがって、分子動力学計算により得られたgp120全長単量体モデルは、動的性質から受容体結合後の構造変化も説明できる機能構造を表していると考えられる。

HIV-1 gp120の大きくゆらぐ部位を知るためにRMSFを調べると、V1/V2領域やV3領域のゆらぎが大きかった。さらに、内側ドメインのゆらぎは外側ドメインよりも大きいことが示唆された。このゆらぎの役割について検討する。Y.D. Kongらによると、gp120はCD4結合構造が基底状態であるが、その構造になる性質はV1/V2領域およびV3領域により制約され、CD4結合していない時は構造的平衡状態にある（PNAS, 109:5663-8, 2012.)。すなわち、V1/V2領域およびV3領域はgp120が基底状態とならないように制約する。この制約がV1/V2領域やV3領域のゆらぎの働きであり、抗体などから逃れるために可塑性を維持する意味があると考えられる。また、V1/V2領域やV3領域のゆらぎや内側ドメインのゆらぎは、CD4結合後の構造変化を誘起するためにも必要であると考えられる。実際、CD4結合後もっとも構造変化する部位はV1/V2領域、V3領域および内側ドメインである。

最後に、抗V3抗体から逃避におけるV1/V2領域の役割について検討する。分子動力学計算により得られたgp120全長単量体モデルは、中和抵抗性株であるJR-FLである。HIV-1 gp120三量体分子モデルより、V3先端は三量体の中心に向かって配置されていた。DCCM解析より、V3領域とV1/V2領域は弱い正の相関運動をしている。V2に位置するR163のCαとV3に位置するG309のCαとの距離の時間変化を調べると、お互いの配置が最適な位置

になるように接近していた。ゆえに、V3領域の配置はV1/V2領域によって影響を受け、V3先端は三量体の中心に向かって配置される。したがって、V1/V2領域はV3領域の配置を制御する重要な役割を持つと考えられる。

## E．結論

HIV-1 gp120 の機能構造を知るため、gp120 全長単量体モデルの分子動力学計算を行い、動的性質を調べた。動的性質は、V1/V2 領域、V3 領域、β20/β21 ループなどの運動が相関していることを示唆していた。三量体モデルより、V3 先端が三量体の中心に向かって配置され、抗 V3 抗体が結合できないことが示唆された。

## F．研究発表

1　論文発表

(1) Yokoyama M, Naganawa S, Yoshimura K, Matsushita S, Sato H. Structural Dynamics of HIV-1 Envelope 1 Gp120 Outer Domain with V3 Loop. PLoS ONE 7: e37530, 2012.

(2) Mori M, Matsuki K, Maekawa T, Tanaka M, Sriwanthana B, Yokoyama M, Ariyoshi K. Development of a Novel In Silico Docking Simulation Model for the Fine HIV-1 Cytotoxic T Lymphocyte Epitope Mapping. PLoS ONE 7: e41703, 2012.

(3) Miyamoto T, Nakayama EE, Yokoyama M, Ibe S, Takehara1 S, Kono K, Yokomaku Y, Pizzato M, Luban J, Sugiura W, Sato H, Shioda T. The carboxyl-terminus of human immunodeficiency virus type 2 circulating recombinant form 01_AB capsid protein affects sensitivity to human TRIM5α. PLoS ONE 7: e47757, 2012.

(4) Nomaguchi M, Yokoyama M, Kono K, Nakayama EE, Shioda T, Saito A, Akari H, Yasutomi Y, Matano T, Sato H, Adachi A. Gag-CA Q110D mutation elicits TRIM5-independent enhancement of HIV-1mt replication in macaque cells. Microbes Infect. 15:56-65, 2013. (The first two authors contributed equally)

2　学会発表

(1) 横山 勝、佐藤 裕徳. 分子動力学計算による HIV-1 gp120 の構造解析. 第 60 回日本ウイルス学会学術集会, 大阪, 2012.

(2) 横山 勝、佐藤 裕徳. HIV-1 gp120 における V1/V2 ドメインと V3 ドメインの配置. 第 26 回日本エイズ学会学術集会・総会, 横浜, 2012.

(3) 横山 勝、佐藤 裕徳. HIV-1 gp120 分子モデルにより示唆される中和逃避メカニズム.第 35 回日本分子生物学会年会, ワークショップ, 福岡, 2012.

## G．知的財産権の出願・登録状況（予定を含む。）

1　特許取得

なし。

2　実用新案登録

なし。

3　その他

なし。

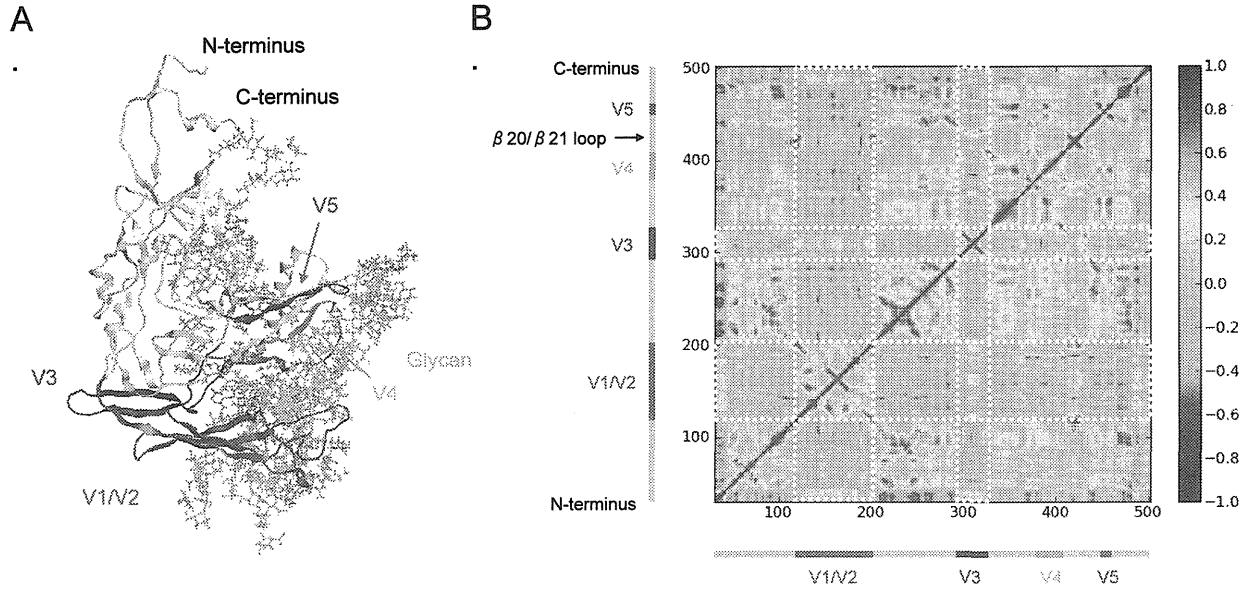


図１． HIV-1 gp120 全長単量体分子モデル(A)と gp120 全長単量体の DCCM 解析により得られた分散共分散行列(B）。

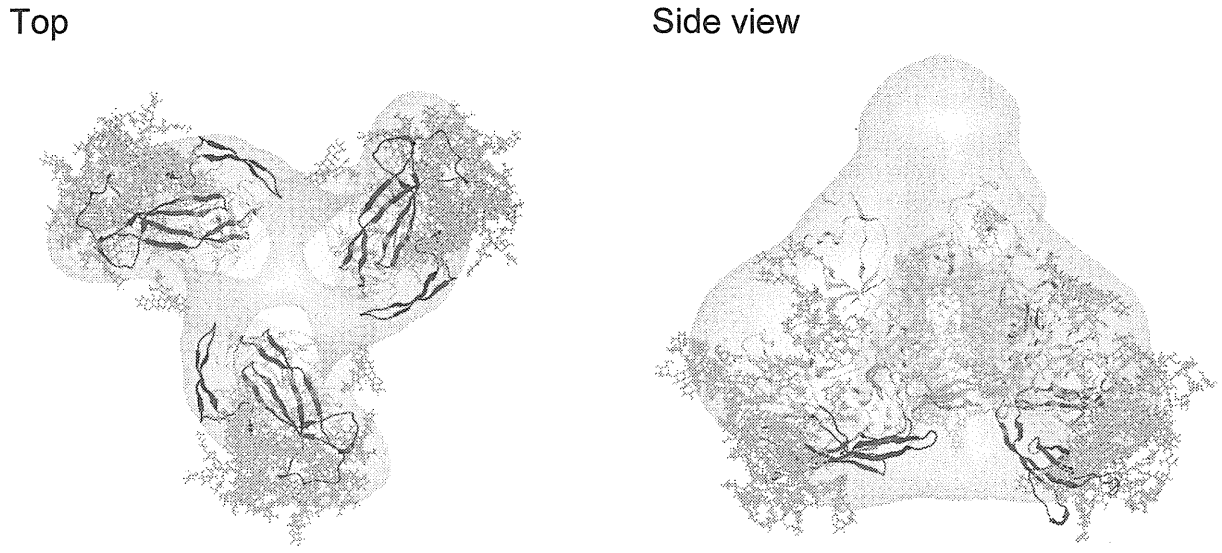


図２． HIV-1 gp120 全長三量体分子モデル。分子動力学計算により得た HIV-1 gp120 全長単量愛分子モデルを、クライオ電子顕微鏡法により得られた構造に重ね合わせることにより構築した。赤いリボン表示は V1/V2 領域、青いリボン表示は V3 領域を示す。

厚生労働科学研究費補助金（エイズ対策研究事業）
分担研究報告書

# 機能的Tリンパ球反応に関する研究

研究分担者　寺原　和孝　国立感染症研究所　免疫部　主任研究官
研究協力者　光木　裕也　国立感染症研究所　免疫部　エイズ予防財団 RR

**研究要旨**

HIV 感染制御における T リンパ球の役割を明らかにするためには、ウイルス制御に関連した機能パラメータの同定が重要であると考えられる。本研究は SIV 感染サルモデルにおける解析を中心とし、ウイルス制御における T リンパ球の機能を明らかにすることを目的とする。H24 年度は急性感染期（wk1）に焦点を当て、ウイルス制御に関連した SIV 特異的 T リンパ球の機能について、Gag 発現センダイウイルスワクチン接種・非接種群間での比較を行った。具体的には末梢血単核球由来 T リンパ球に対して SIV 抗原刺激を行い、5 種類のエフェクター因子（MIP-1β, IL-2, TNF-α, IFN-γ, CD107 a ）の発現能をフローサイトメトリーにて解析した。その結果、ワクチン接種群においては total（上記 5 種類のエフェクター因子のうち少なくともいずれかを発現するもの）／IFN-$\gamma^+$／CD107a$^+$ CD4 陽性 T リンパ球の頻度が血中ウイルス量と有意な逆相関を示した。。一方、ワクチン非接種群において血中ウイルス量と有意な逆相関を示したのは、IFN-$\gamma^+$／MIP-1$\beta^+$ CD4 陽性 T リンパ球、ならびに total ／MIP-1$\beta^+$ CD8 陽性 T リンパ球の頻度であった。以上の結果から、ワクチン接種の有無や T リンパ球サブセットの違いによってウイルス制御に関連した T リンパ球の機能パターンが異なることが示された。

## A．研究目的

CD8 陽性細胞傷害性 T リンパ球（CTL）は、慢性持続感染を成立させる HIV および SIV の体内複製制御において中心的役割を担う。一方、CD4 陽性ヘルパーT リンパ球は、CTL の誘導・維持に重要であるとされつつもそれ自身が HIV の標的であることから、HIV 感染制御における役割についてはいまだ不明な点が多い。そこで本研究では、HIV 感染制御におけるウイルス抗原特異的 T リンパ球の免疫学的機能を明らかにすることを目的とした。このことは、俣野らが中心となって進めている Gag 発現センダイウイルス（SeV-Gag）をベースとした CTL 誘導型エイズワクチンの有効性に対する科学的根拠を提示するうえでも重要な課題であると考えられる。

これまで、本研究分担者による SIV 感染サルの慢性持続感染期を対象にした解析において、IL-2 発現能を有する SIV 特異的 CD4 T リンパ球の頻度がウイルス制御と関連することが見いだされた。そこで本年度は、急性感染期に遡り、ウイルス制御に関連する T リンパ球の機能パラメータの同定を試みた。

## B．研究方法

本解析に供したビルマ産アカゲサルを表 1 に示す。SIVmac239 チャレンジ後 1 週の末梢血由来単核球と VSV-G シュードタイプ SIV を感染させた同一個体由来の B lymphoblastoid cell line（SIV-BLCL）を共培養後、CD4 陽性および CD8 陽性 T リンパ球における MIP-1β, IL-2, TNF-α, IFN-γ, CD107 a の発現をフローサイトメトリーにて解析した。

（倫理面への配慮）

遺伝子組換え生物等を用いる実験については、国立感染症研究所の承認あるいは文部科学大臣の確認を得て行った。

表 1. 解析に供したビルマ産アカゲサル

| ワクチン接種群 | | ワクチン非接種群 | |
|---|---|---|---|
| MHC-Iハプロタイプ | 個体数 | MHC-Iハプロタイプ | 個体数 |
| A | 3 | A | 4 |
| D | 4 | D | 5 |
| E | 5 | E | 7 |
| B | 1 | B | 5 |
| J | 4 | J | 5 |

ワクチン接種は SeV-Gag による。

## C．研究結果

### 1) ワクチン接種群におけるSIV特異的Tリンパ球反応

ウイルスチャレンジ後1週目のSIV特異的Tリンパ球の頻度と血中ウイルス量との相関を解析した結果、total（5種類のエフェクター因子のうち、いずれかを発現するもの）、ならびに、IFN-γあるいはCD107a発現能を有するSIV特異的CD4陽性Tリンパ球の頻度が血中ウイルス量に対して有意な逆相関を示した（図1）。

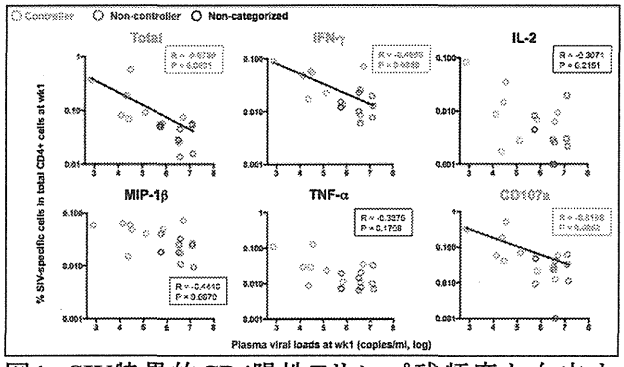


**図1. SIV特異的CD4陽性Tリンパ球頻度と血中ウイルス量との相関（ワクチン接種群：急性期wk1）**

一方、SIV特異的CD8陽性Tリンパ球についても同様に解析した結果、血中ウイルス量に対して有意な逆相関を示す細胞群は認められなかった。

### 2) ワクチン非接種群におけるSIV特異的Tリンパ球反応

ワクチン非接種群についても同様に解析した結果、まずSIV特異的CD4陽性Tリンパ球についてはIFN-γあるいはMIP-1β発現能を有する細胞頻度が血中ウイルス量に対して有意な逆相関を示した（図2）。

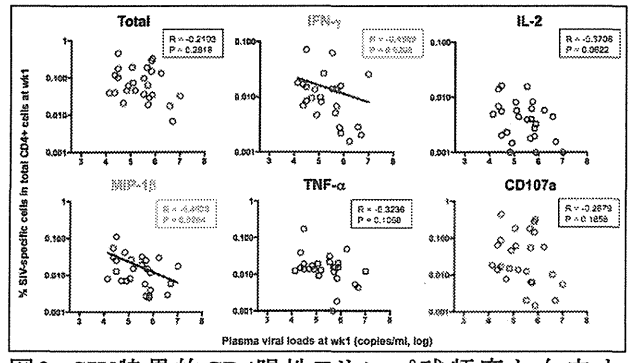


**図2. SIV特異的CD4陽性Tリンパ球頻度と血中ウイルス量との相関（ワクチン非接種群：急性期wk1）**

さらに、SIV 特異的 CD8 陽性 T リンパ球についてみたところ、total ならびに MIP-1β発現能を有する細胞頻度が血中ウイルス量に対して有意な逆相関を示した（図 3）。

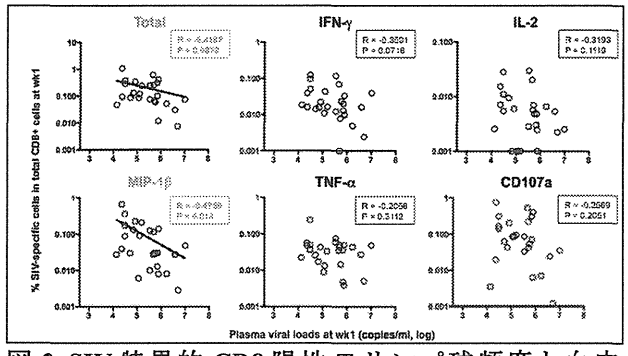


**図 3. SIV 特異的 CD8 陽性 T リンパ球頻度と血中ウイルス量との相関（ワクチン非接種群：急性期 wk1）**

## D．考察

本年度の急性感染期における解析結果から、ワクチン接種の有無によって SIV 特異的 CD4 ならびに CD8 陽性 T リンパ球の機能パターンが異なることが示され、ワクチン接種による免疫賦活がこのような機能パターンの変化に影響を及ぼしたものと考えられた。しかしながら、ワクチン接種の有無、また、T リンパ球サブセットを問わず、ウイルス制御に関連するものとして見出されたエフェクター因子（IFN-γ, MIP-1β, CD107a）の特性から、直接的な抗ウイルス作用を示すものがこの時期の機能的なTリンパ球であることが想像された。

これまでの慢性持続感染期を対象とした先行研究データでは、ワクチン接種の有無を問わず IL-2 発現能を有する SIV 特異的 CD4 陽性 T リンパ球の頻度がウイルス制御と関連することを見出したが、急性感染期ではこのような機能パター

ンとも異なっていた。このことから、ウイルス制御に関連したTリンパ球の機能を明らかにするためにも、ワクチン接種の有無、感染進行度やTリンパ球サブセットの違いに応じた抗原特異的Tリンパ球の機能パターンを明らかにすることが重要である。今回はSIV特異的Tリンパ球の頻度について解析を行ったが、今後は多機能性についても解析を行い、より適切な機能パラメータの同定を目指す。

## E．結論

ウイルス制御と関連するTリンパ球の機能パターンは、ワクチン接種の有無や感染進行度、また、細胞種（CD4/CD8 Tリンパ球）によって異なることが示された。

## F．研究発表

1　論文発表

(1) Terahara K, Ishige M, Ikeno S, Mitsuki Y-y, Okada S, Kobayashi K, Tsunetsugu-Yokota Y. Expansion of activated memory $CD4^+$ T cells affects infectivity of CCR5-tropic HIV-1 in humanized NOD/SCID/$JAK3^{null}$ mice. PLoS One. 8, e53495, 2013.

(2) Tsunetsugu-Yokota Y, Terahara K. (Editor Article) Receptor usage and the pathogenesis in acute and chronic virus infections. Front. Microbiol. 3, 289, 2012.

(3) Mitsuki Y-y, Terahara K, Shibusawa K, Yamamoto T, Tsuchiya T, Mizukoshi F, Ishige M, Okada S, Kobayashi K, Morikawa Y, Nakayama T, Takeda M, Yanagi Y, Tsunetsugu-Yokota Y. HIV-1 infection *ex vivo* accelerates measles virus infection by upregulating signaling lymphocytic activation molecule (SLAM) in $CD4^+$ T cells. J. Virol. 86, 7227-7234, 2012.

(4) Nomura T, Yamamoto H, Shiino T, Takahashi N, Nakane T, Iwamoto N, Ishii H, Tsukamoto T, Kawada M, Matsuoka S, Takeda A, Terahara K, Tsunetsugu-Yokota Y, Iwata-Yoshikawa N, Hasegawa H, Sata T, Naruse T, Kimura A, Matano T. Association of major histocompatibility complex class I haplotypes with disease progression after simian immunodeficiency virus challenge in Burmese rhesus macaques. J. Virol. 86, 6481-6490, 2012.

2　学会発表

(1) 鈴木基臣、モリテツシ、寺原和孝、横田（恒次）恭子、竹山春子：キャピラリープレートを用いた単一細胞解析のためのデジタル PCR 法の開発とHIV 研究へのアプローチ、第 6 回バイオ関連化学シンポジウム、札幌、2012 年 9 月

(2) 池野翔太、寺原和孝、石毛真行、鈴木基臣、光木裕也、森川裕子、中川哲夫、横田恭子：ヒト化マウスの麻疹ウイルスベクター評価系への応用、第 60 回日本ウイルス学会学術集会、大阪、2012 年 11 月

(3) Tsunetsugu-Yokota Y, Ishige M, Ikeno S, Terahara K. Humanized mice as an animal model for human-tropic virus infection. Immunological Mechanisms of Vaccination, Keystone Symposia, Ottawa, Ontario, Canada, Dec 13-18, 2012.

## G．知的財産権の出願・登録状況（予定を含む。）

1　特許取得

なし。

2　実用新案登録

なし。

3　その他

なし。

# Ⅲ．　研究成果の刊行に関する一覧表

研究成果の刊行に関する一覧表

雑誌

| 発表者氏名 | 論文タイトル名 | 発表誌名 | 巻号 | ページ | 出版年 |
|---|---|---|---|---|---|
| Nomura T, Yamamoto H, Shiino T, Takahashi N, Nakane T, Iwamoto N, Ishii H, Tsukamoto T, Kawada M, Matsuoka S, Takeda A, Terahara K, Tsunetsugu-Yokota Y, Iwata-Yoshikawa N, Hasegawa H, Sata T, Naruse TK, Kimura A, Matano T. | Association of major histocompatibility complex class I haplotypes with disease progression after simian immunodeficiency virus challenge in Burmese rhesus macaques. | J Virol | 86 | 6481-6490 | 2012 |
| Tee KK, Kamarulzaman A, Matano T, Takebe Y. | Phylodynamic inference of infectious diseases caused by the human immunodeficiency virus, enterovirus 71, and the 2009 swine-origin human influenza virus. | Future Virol | 7 | 403-412 | 2012 |
| Ohtani H, Naruse TK, Iwasaki Y, Akari H, Ishida T, Matano T, Kimura A. | Lineage-specific evolution of T-cell immunoglobulin and mucin domain 1 gene in the primates. | Immunogenetics | 64 | 669-678 | 2012 |
| Nomura T, Matano T. | Association of MHC-I genotypes with disease progression in HIV/SIV infections. | Front Microbiol | 3 | 234 | 2012 |
| Kurihara K, Takahara Y, Nomura T, Ishii H, Iwamoto N, Takahashi N, Inoue M, Iida A, Hara H, Shu T, Hasegawa M, Moriya C, Matano T. | Immunogenicity of repeated Sendai viral vector vaccination in macaques. | Microbes Infect | 14 | 1169-1176 | 2012 |
| Takahashi N, Nomura T, Takahara Y, Yamamoto H, Shiino T, Takeda A, Inoue M, Iida A, Hara H, Shu T, Hasegawa M, Sakawaki H, Miura T, Igarashi T, Koyanagi Y, Naruse TK, Kimura A, Matano T. | A novel protective MHC-I haplotype not associated with dominant Gag-specific CD8+ T-cell responses in SIVmac239 infection of Burmese rhesus macaques. | PLoS ONE | 8 | e54300 | 2013 |
| Kondo M, Lemey P, Sano T, Itoda I, Yoshimura Y, Sagara H, Tachikawa N, Yamanaka K, Iwamuro S, Matano T, Imai M, Kato S, Takebe Y. | Emergence in Japan of an HIV-1 variant associated with MSM transmission in China: First indication for the international dissemination of the Chinese MSM lineage. | J Virol | | in press | |
| Karamatsu K, Matsuo K, Inada H, Tsujimura Y, Shiogama Y, Matsubara A, Kawano M, Yasutomi Y. | Single systemic administration of Ag85B of mycobacteria DNA inhibits allergic airway inflammation in a mouse model of asthma. | J Asthma Allergy | 5 | 71-79 | 2012 |

| | | | | | |
|---|---|---|---|---|---|
| Tajiri K, Imanaka-Yoshida K, Matsubara A, Tsujimura Y, Hiroe M, Naka T, Shimojo N, Sakai S, Aonuma K, Yasutomi Y. | Suppressor of cytokine signaling 1 (SOCS1) DNA administration inhibits inflammatory and pathogenic responses in autoimmune myocarditis. | J Immunol | 189 | 2043-2053 | 2012 |
| Higashino A, Sakate R, Kameoka Y, Takahashi I, Hirata M, Tanuma R, Masui T, Yasutomi Y, Osada N. | Whole-genome sequencing and analysis of the Malaysian cynomolgus macaque (Macaca fascicularis) genome. | Genome Biol | 13 | R58 | 2012 |
| Tachibana S, Sullivan SA, Kawai S, Nakamura S, Goto N, Arisue N, Palacpac NMQ, Honma H, Yagi M, Tougan T, Katakai Y, Kaneko O, Mita T, Kita K, Yasutomi Y, Kim HR, Sutton PL, Shakhbatyan R, Horii T, Yasunaga T, Bamwell JW, Escalante AA, Carlton JM, Tanabe K. | Plasmodium cynomolgi genome sequences provide insight into Plasmodium vivax and the monkey malaria clade. | Nature Genetics | 44 | 1051-1055 | 2012 |
| Yoshhida T, Omatsu T, Saito A, Katakai Y, Iwasaki, Y, Kurosawa T, Hamano M, Higashimo A, Nakamura S, Takasaki T, Yasutomi Y, Kurane I, Akari H. | Dynamics of cellular immune responses in the acute phase of dengue virus infection. | Archiv Virol | | in press | |
| Tougan T, Aoshi T, Coban C, Katakai Y, Kai C, Yasutomi Y, Ishii KJ, Horii T. | TLR9 adjuvants enhance immunogenicity and protective efficacy of the SE36/AHG malaria vaccine in nonhuman primate models. | Hum Vac Immunother | | in press | |
| Haraguchi H, Noda T, Kawaoka Y, Morikawa Y. | A large extension to HIV-1 Gag, like Pol, has negative impacts on virion assembly. | PLOS One | 7 | e47828 | 2012 |
| Sudo S, Haraguchi H, Hirai Y, Gatanaga H, Sakuragi J-I, Momose F, Morikawa Y. | Efavirenz enhances HIV-1 Gag processing at the plasma membrane through Gag-Pol dimerization. | J Virol | | in press | |
| Shinohara M, Io K, Shindo K, Matsui M, Sakamoto T, Tada K, Kobayashi M, Kadowaki N, Takaori-Kondo A. | APOBEC3B can impair genomic stability by inducing base substitutions in genomic DNA in human cells. | Sci Rep | 2, 806 | 1-9 | 2012 |
| Fujita H, Kitawaki T, Sato T, Maeda T, Kamihira S, Takaori-Kondo A, Kadowaki N. | The tyrosine kinase inhibitor dasatinib suppresses cytokine production by plasmacytoid dendritic cells by targeting endosomal transport of CpG DNA. | Eur J Immunol | 43 | 93-103 | 2012 |

| | | | | | |
|---|---|---|---|---|---|
| Furukawa A, Okamura H, Morishita R, Matsunaga S, Kobayashi N, Ikegami T, Kodaki T, Takaori-Kondo A, Ryo A, Nagata T, Katahira M. | NMR study of xenotropic murine leukemia virus-related virus protease in a complex with amprenavir. | Biochem Biophys Res Commun | 425 | 284-289 | 2012 |
| Matsunaga S, Sawasaki T, Ode H, Morishita R, Furukawa A, Sakuma R, Sugiura W, Sato H, Katahira M, Takaori-Kondo A, Yamamoto N, Ryo A. | Molecular and enzymatic characterization of XMRV protease by a cell-free proteolytic analysis. | J Proteomics | 75 | 4863-4873 | 2012 |
| Chonabayashi K, Hishizawa M, Kawamata S, Nagai Y, Ohno T, Ishikawa T, Uchiyama T, Takaori-Kondo A. | Direct binding of Grb2 has an important role in the development of myeloproliferative disease induced by ETV6/FLT3. | Leukemia | | in press | |
| Ong YT, Kirby KA, Hachiya A, Chiang LA, Marchand B, Yoshimura K, Murakami T, Singh K, Matsushita S, Sarafianos SG. | Preparation of biologically active single-chain variable antibody fragments that target the HIV-1 gp120 V3 loop. | Cell Mol Biol | 58 | 71-79 | 2012 |
| Harada S, Yoshimura K, Yamaguchi A, Boonchawalit S, Yusa K, Matsushita S. | Impact of antiretroviral pressure on selection of primary HIV-1 envelope sequences in vitro. | J Gen Virol | | in press | |
| Yokoyama M, Naganawa S, Yoshimura K, Matsushita S, Sato H. | Structural Dynamics of HIV-1 Envelope 1 Gp120 Outer Domain with V3 Loop. | PLoS ONE | 7 | e37530 | 2012 |
| Mori M, Matsuki K, Maekawa T, Tanaka M, Sriwanthana B, Yokoyama M, Ariyoshi K. | Development of a Novel In Silico Docking Simulation Model for the Fine HIV-1 Cytotoxic T Lymphocyte Epitope Mapping. | PLoS ONE | 7 | e41703 | 2012 |
| Miyamoto T, Nakayama EE, Yokoyama M, Ibe S, Takehara1 S, Kono K, Yokomaku Y, Pizzato M, Luban J, Sugiura W, Sato H, Shioda T. | The carboxyl-terminus of human immunodeficiency virus type 2 circulating recombinant form 01_AB capsid protein affects sensitivity to human TRIM5α. | PLoS ONE | 7 | e47757 | 2012 |
| Nomaguchi M, Yokoyama M, Kono K, Nakayama EE, Shioda T, Saito A, Akari H, Yasutomi Y, Matano T, Sato H, Adachi A. | Gag-CA Q110D mutation elicits TRIM5-independent enhancement of HIV-1mt replication in macaque cells. | Microbes Infect | 15 | 56-65 | 2013 |
| Tsunetsugu-Yokota Y, Terahara K. | Receptor usage and the pathogenesis in acute and chronic virus infections. | Front Microbiol | 3 | 289 | 2012 |
| Mitsuki Y-y, Terahara K, Shibusawa K, Yamamoto T, Tsuchiya T, Mizukoshi F, Ishige M, Okada S, Kobayashi K, Morikawa Y, Nakayama T, Takeda M, Yanagi Y, Tsunetsugu-Yokota Y. | HIV-1 infection *ex vivo* accelerates measles virus infection by upregulating signaling lymphocytic activation molecule (SLAM) in $CD4^+$ T cells. | J Virol | 86 | 7227-7234 | 2012 |

| | | | | | |
|---|---|---|---|---|---|
| Terahara K, Ishige M, Ikeno S, Mitsuki Y-y, Okada S, Kobayashi K, Tsunetsugu-Yokota Y. | Expansion of activated memory $CD4^+$ T cells affects infectivity of CCR5-tropic HIV-1 in humanized NOD/SCID/$JAK3^{null}$ mice. | PLoS One | 8 | e53495 | 2013 |

# Ⅳ.　研究成果の刊行物・別刷

JVI Journals.ASM.org

# Association of Major Histocompatibility Complex Class I Haplotypes with Disease Progression after Simian Immunodeficiency Virus Challenge in Burmese Rhesus Macaques

Takushi Nomura,[a,b] Hiroyuki Yamamoto,[a] Teiichiro Shiino,[a] Naofumi Takahashi,[a,b] Taku Nakane,[a,b] Nami Iwamoto,[a,b] Hiroshi Ishii,[a,b] Tetsuo Tsukamoto,[b] Miki Kawada,[b] Saori Matsuoka,[a] Akiko Takeda,[a] Kazutaka Terahara,[c] Yasuko Tsunetsugu-Yokota,[c] Naoko Iwata-Yoshikawa,[d] Hideki Hasegawa,[d] Tetsutaro Sata,[d] Taeko K. Naruse,[e] Akinori Kimura,[e] and Tetsuro Matano[a,b]

AIDS Research Center, National Institute of Infectious Diseases, Toyama, Shinjuku-ku, Tokyo, Japan[a]; The Institute of Medical Science, The University of Tokyo, Shirokanedai, Minato-ku, Tokyo, Japan[b]; Department of Immunology, National Institute of Infectious Diseases, Toyama, Shinjuku-ku, Tokyo, Japan[c]; Department of Pathology, National Institute of Infectious Diseases, Toyama, Shinjuku-ku, Tokyo, Japan[d]; and Department of Molecular Pathogenesis, Medical Research Institute, Tokyo Medical and Dental University, Kandasurugadai, Chiyoda-ku, Tokyo, Japan[e]

**Nonhuman primate AIDS models are essential for the analysis of AIDS pathogenesis and the evaluation of vaccine efficacy. Multiple studies on human immunodeficiency virus and simian immunodeficiency virus (SIV) infection have indicated the association of major histocompatibility complex class I (MHC-I) genotypes with rapid or slow AIDS progression. The accumulation of macaque groups that share not only a single MHC-I allele but also an MHC-I haplotype consisting of multiple polymorphic MHC-I loci would greatly contribute to the progress of AIDS research. Here, we investigated SIVmac239 infections in four groups of Burmese rhesus macaques sharing individual MHC-I haplotypes, referred to as A, E, B, and J. Out of 20 macaques belonging to $A^+$ ($n = 6$), $E^+$ ($n = 6$), $B^+$ ($n = 4$), and $J^+$ ($n = 4$) groups, 18 showed persistent viremia. Fifteen of them developed AIDS in 0.5 to 4 years, with the remaining three at 1 or 2 years under observation. $A^+$ animals, including two controllers, showed slower disease progression, whereas $J^+$ animals exhibited rapid progression. $E^+$ and $B^+$ animals showed intermediate plasma viral loads and survival periods. Gag-specific $CD8^+$ T-cell responses were efficiently induced in $A^+$ animals, while Nef-specific $CD8^+$ T-cell responses were in $A^+$, $E^+$, and $B^+$ animals. Multiple comparisons among these groups revealed significant differences in survival periods, peripheral $CD4^+$ T-cell decline, and SIV-specific $CD4^+$ T-cell polyfunctionality in the chronic phase. This study indicates the association of MHC-I haplotypes with AIDS progression and presents an AIDS model facilitating the analysis of virus-host immune interaction.**

Virus-specific $CD8^+$ cytotoxic T lymphocytes (CTLs) are major effectors against persistent virus infections (13, 44). In virus-infected cells, viral antigen-derived peptides (epitopes) are bound to major histocompatibility complex class I (MHC-I) molecules and presented on the cell surface. Viral peptide-specific CTLs recognize the peptide-MHC-I complexes by their T-cell receptors. CTL effectors deliver cell death via apoptosis as well as lysis (15, 48).

Human immunodeficiency virus type 1 (HIV-1) infection induces persistent viral replication leading to AIDS progression. CTL responses play a central role in the suppression of HIV-1 replication (6, 18, 25, 32, 43). Multiple studies on HIV-1-infected individuals have shown an association of HLA genotypes with rapid or delayed AIDS progression (14, 23, 27, 51, 54). For instance, HIV-1-infected individuals possessing *HLA-B*57* tend to show a better prognosis with lower viral loads, implicating HLA-B*57-restricted epitope-specific CTL responses in this viral control (3, 33, 34). In contrast, the association of *HLA-B*35* with rapid disease progression has been indicated (8).

Nonhuman primate AIDS models are important for the analysis of AIDS pathogenesis and the evaluation of vaccine efficacy (5, 35, 47). Models of simian immunodeficiency virus (SIV) infection in macaques are widely used currently (12, 22). Indian rhesus macaques possessing certain MHC-I alleles, such as *Mamu-A*01*, *Mamu-B*08*, and *Mamu-B*17*, tend to show lower set point plasma viral loads in SIV infection (30, 36, 37, 59). Regarding MHC-I alleles, humans have a single polymorphic HLA-A, HLA-B, and HLA-C locus per chromosome, whereas MHC-I haplotypes in macaques have variable numbers of expressed polymorphic MHC-I loci (7, 9, 26, 41). Thus, the accumulation of multiple macaque groups, each sharing a different MHC-I haplotype, would contribute to the precise analysis of SIV infection.

We have been working on the establishment of an AIDS model using Burmese rhesus macaques sharing MHC-I haplotypes (38, 50). In the present study, we have focused on SIV infection in four groups of Burmese rhesus macaques, each consisting of four or more animals. These groups share MHC-I haplotypes *90-120-Ia* (referred to as A), *90-010-Ie* (E), *90-120-Ib* (B), and *90-088-Ij* (J), respectively. The analysis of SIVmac239 infection among these groups revealed differences in plasma viral loads, peripheral $CD4^+$ T cell counts, survival periods, virus-specific CTL responses, and T-cell polyfunctionality. Our results indicate the association of MHC-I haplotypes with disease progression in SIV infection and present a sophisticated model of SIV infection.

Received 11 December 2011 Accepted 27 March 2012
Published ahead of print 4 April 2012
Address correspondence to Tetsuro Matano, tmatano@nih.go.jp.

doi:10.1128/JVI.07077-11

TABLE 1 MHC-I haplotypes

| MHC-I haplotype | Confirmed MHC-I allele(s) | |
|---|---|---|
| | *Mamu-A* | *Mamu-B* |
| A (*90-120-Ia*) | *A1*043:01, A1*065:01* | *B*061:03, B*068:04, B*089:01* |
| E (*90-010-Ie*) | *A1*066:01* | *B*005:02, B*015:04* |
| B (*90-120-Ib*) | *A1*018:08, A2*005:31* | *B*036:03, B*037:01, B*043:01, B*162:01* |
| J (*90-088-Ij*) | *A1*008:01* | *B*007:02, B*039:01* |

## MATERIALS AND METHODS

**Animal experiments.** We examined SIV infections in four groups of Burmese rhesus macaques having MHC-I haplotypes *90-120-Ia* (A) ($n$ = 6), *90-010-Ie* (E) ($n$ = 6), *90-120-Ib* (B) ($n$ = 4), and *90-088-Ij* (J) ($n$ = 4). Macaques R02-007, R06-037, R07-001, R07-004, R07-009, R01-011, R06-038, R06-001, R02-004, R04-014, and R06-022, which were used as controls in previous experiments (49, 53, 58), were included in the present study. The determination of MHC-I haplotypes was based on the family study in combination with the reference strand-mediated conformation analysis (RSCA) of *Mamu-A* and *Mamu-B* genes as described previously (31). Briefly, locus-specific reverse transcription-PCR (RT-PCR) products from total cellular RNAs were prepared and used to form heteroduplex DNAs with a 5′ Cy5-labeled reference strand (50). The heteroduplex DNAs were subjected to a 6% nondenaturing acrylamide gel electrophoresis to identify the patterns of MHC-I haplotypes. In addition, although recombination events could not be ruled out, major *Mamu-A* and *Mamu-B* alleles were determined by cloning the RT-PCR products and sequencing at least 48 clones for each locus from each subject as described previously (38). Because we used locus-specific primers in the RT-PCR, which were designed on the basis of known alleles (31, 38), MHC class I alleles harboring mismatches with the primer sequences or alleles of low expression would not be amplified well, hence there was a limitation that not all of the MHC class I alleles could be detected in our study. Confirmed *Mamu-A* and *Mamu-B* alleles in MHC-I haplotypes A, E, B, and

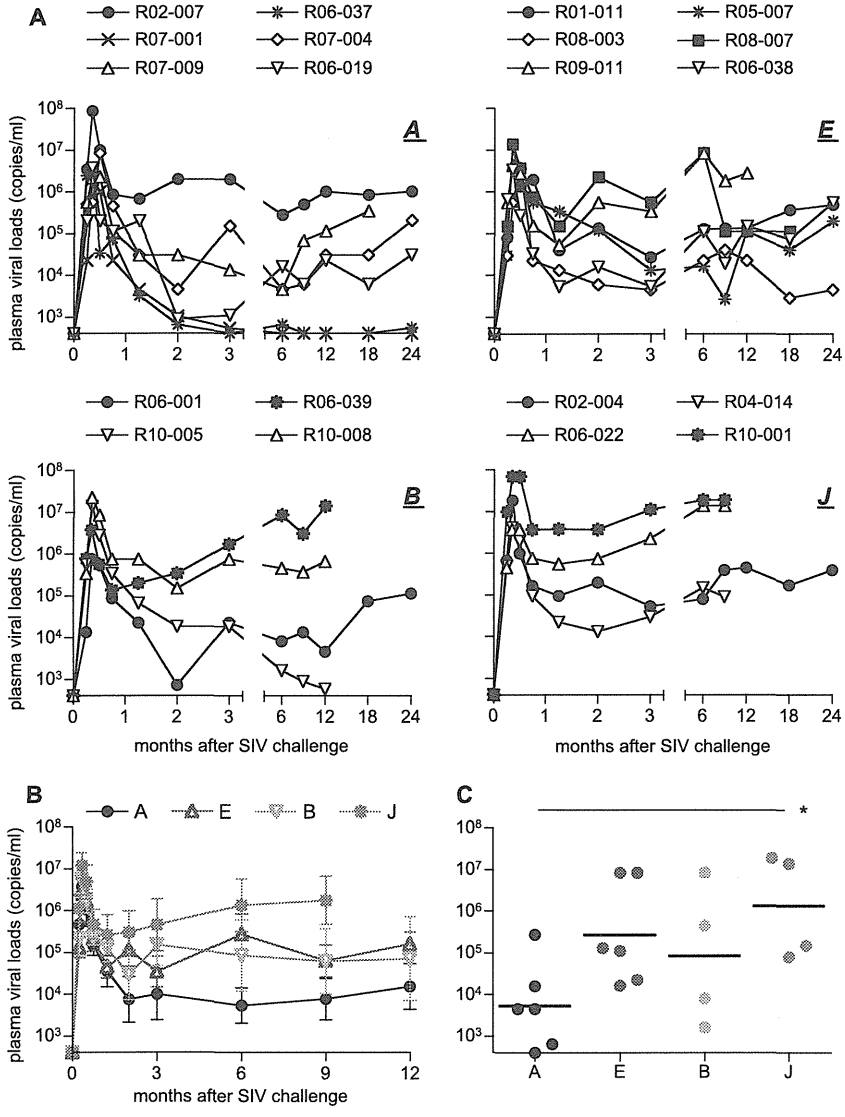


FIG 1 Plasma viral loads after SIVmac239 challenge. Plasma viral loads (SIV *gag* RNA copies/ml plasma) were determined as described previously (31). The lower limit of detection is approximately $4 \times 10^2$ copies/ml. (A) Changes in plasma viral loads after challenge in $A^+$ (upper left), $E^+$ (upper right), $B^+$ (lower left), and $J^+$ (lower right) macaques. (B) Changes in geometric means of plasma viral loads after challenge in $A^+$ (black), $E^+$ (blue), $B^+$ (green), and $J^+$ (red) animals. (C) Comparison of plasma viral loads at 6 months among four groups. Those of $A^+$ animals were significantly lower than those of $J^+$ animals ($P$ = 0.0444 by one-way ANOVA and Tukey-Kramer's multiple-comparison test).

J are shown in Table 1 (38). All animals were unvaccinated and challenged intravenously with 1,000 $TCID_{50}$ (50% tissue culture infective doses) of SIVmac239 (22). At 1 week after challenge, macaques R06-019, R06-038, and R10-008 were intravenously infused with 300 mg of nonspecific immunoglobulin G purified from uninfected rhesus macaques (57). Fifteen animals were euthanized when they showed typical signs of AIDS, such as reduction in peripheral $CD4^+$ T-cell counts, loss of body weight, diarrhea, and general weakness. Autopsy revealed lymphoatrophy or postpersistent generalized lymphadenopathy conditions consistent with AIDS (20). All animals were maintained in accordance with the guidelines for animal experiments at the National Institute of Biomedical Innovation and National Institute of Infectious Diseases.

**Analysis of SIV antigen-specific $CD8^+$ T-cell responses.** SIV antigen-specific $CD8^+$ T-cell responses were measured by the flow-cytometric analysis of gamma interferon (IFN-γ) induction as described previously (17). Peripheral blood mononuclear cells (PBMCs) were cocultured with autologous herpesvirus papioimmortalized B-lymphoblastoid cell lines (B-LCLs) pulsed with peptide pools using panels of overlapping peptides spanning the entire SIVmac239 Gag, Pol, Vif, Vpx, Vpr, Tat, Rev, Env, and Nef amino acid sequences. Intracellular IFN-γ staining was performed using a Cytofix Cytoperm kit (BD, Tokyo, Japan). Fluorescein isothiocyanate-conjugated anti-human CD4 (BD), peridinin chlorophyll protein (PerCP)-conjugated anti-human CD8 (BD), allophycocyanin Cy7 (APC-Cy7)-conjugated anti-human CD3 (BD), and phycoerythrin (PE)-conjugated anti-human IFN-γ antibodies (Biolegend, San Diego, CA) were used. Specific T-cell levels were calculated by subtracting nonspecific IFN-$\gamma^+$ T-cell frequencies from those after peptide-specific stimulation. Specific T-cell levels of less than 100 cells per million PBMCs were considered negative. Using PBMCs obtained from four SIV-infected macaques, we compared antigen-specific $CD8^+$ T-cell frequencies measured by this method (using peptide-pulsed B-LCLs) to those measured by the flow-cytometric analysis of IFN-γ induction after a pulse of PBMCs with peptides (without using B-LCLs). The levels of the former tended to be slightly higher than those of the latter. Specific $CD8^+$ T-cell responses, which were shown to be 100 to 200 cells per million PBMCs by the former method using B-LCLs, were undetectable by the latter method.

**Sequencing analysis of plasma viral genomes.** Viral RNAs were extracted using the High Pure Viral RNA kit (Roche Diagnostics, Tokyo, Japan) from macaque plasma obtained around 1 year after challenge. Fragments of cDNAs encoding SIVmac239 Gag, Pol, Vif, Vpx, Vpr, Tat, Rev, and Nef were amplified by nested RT-PCR from plasma RNAs and subjected to direct sequencing by using dye terminator chemistry and an automated DNA sequencer (Applied Biosystems, Tokyo, Japan) as described before (19). Predominant nonsynonymous mutations were determined. The Env-coding region, which is known to have multiple antibody-related mutations, was not included for the analysis.

**Analysis of SIV-specific polyfunctional T-cell responses.** To analyze polyfunctionality in SIV-specific T-cell responses, we examined the SIV-specific induction of IFN-γ, tumor necrosis factor alpha (TNF-α), interleukin-2 (IL-2), macrophage inflammatory protein 1β (MIP-1β), and CD107a in $CD4^+$ and $CD8^+$ T cells as described previously (58), with some modifications. Around 8 months after challenge, PBMCs were cocultured with B-LCLs infected with vesicular stomatitis virus G protein-pseudotyped SIVGP1 for the SIV-specific stimulation or mock-infected B-LCLs for nonspecific stimulation. The pseudotyped virus was obtained by the cotransfection of 293T cells with a vesicular stomatitis virus G protein expression plasmid and an *env* and *nef* deletion-containing simian-human immunodeficiency virus molecular clone (SIVGP1) DNA that has the genes encoding SIVmac239 Gag, Pol, Vif, Vpx, and a part of Vpr (31, 46). Immunostaining was performed using a Fix & Perm fixation and permeabilization kit (Invitrogen, Tokyo, Japan) and the following monoclonal antibodies: APC-Cy7-conjugated anti-human CD3 (BD), PE-Texas red-conjugated anti-human CD4 (Invitrogen), Alexa Fluor 700-conjugated anti-human CD8 (BD), PE-Cy7-conjugated anti-human IFN-γ (eBioscience, San Diego, CA), Pacific blue-conjugated anti-human TNF-α (Biolegend), PerCP-Cy5.5-conjugated anti-human IL-2 (Biolegend), PE-conjugated anti-human MIP-1β (BD), and Alexa Fluor 647-conjugated anti-human CD107a (Biolegend). Dead cells were stained using Live/Dead Fixable Dead Cell Stain kit (Invitrogen). Analysis was carried out using PESTLE (version 1.6.1) and SPICE (version 5.2) programs as described previously (42). The polyfunctionality (polyfunctional value) was shown as mean numbers of induced factors among the five (IFN-γ, TNF-α, IL-2, MIP-1β, and CD107a) per SIV-specific T cell.

**Statistical analysis.** Statistical analyses were performed using R software (R Development Core Team). Comparisons were performed by one-way analysis of variance (ANOVA) and Tukey-Kramer's multiple comparison test with significance levels set at $P < 0.05$. Correlation was analyzed by the Pearson test.

TABLE 2 List of macaques in this study

| MHC-I haplotype | Macaque | Disease progression | Euthanasia time point (mo) |
|---|---|---|---|
| A | R02-007 | AIDS | 42 |
| A | R06-037 | No | 49 |
| A | R07-001 | No | 49 |
| A | R07-004 | AIDS | 40 |
| A | R07-009 | AIDS | 17 |
| A | R06-019 | AIDS | 43 |
| E | R01-011 | AIDS | 24 |
| E | R05-007 | AIDS | 37 |
| E | R08-003 | Under observation (24 months) | |
| E | R08-007 | AIDS | 20 |
| E | R09-011 | AIDS | 12 |
| E | R06-038 | AIDS | 22 |
| B | R06-001 | AIDS | 34 |
| B | R06-039 | AIDS | 13 |
| B | R10-005 | Under observation (12 months) | |
| B | R10-008 | Under observation (12 months) | |
| J | R02-004 | AIDS | 37 |
| J | R04-014 | AIDS | 9 |
| J | R06-022 | AIDS | 5 |
| J | R10-001 | AIDS | 9 |

## RESULTS

**SIV infection in Burmese rhesus macaques.** We accumulated four groups of unvaccinated, SIVmac239-infected Burmese rhesus macaques, groups $A^+$ ($n = 6$), $E^+$ ($n = 6$), $B^+$ ($n = 4$), and $J^+$ ($n = 4$), sharing MHC-I haplotypes A (*90-120-Ia*), E (*90-010-Ie*), B (*90-120-Ib*), and J (*90-088-Ij*), respectively, to compare SIV infections among these groups (Table 1). Out of these 20 animals, 18 showed persistent viremia (geometric mean plasma viral loads at 6 months of $1.6 \times 10^5$ copies/ml), while in the remaining two ($A^+$ macaques R06-037 and R07-001), plasma viral loads became less than $10^3$ copies/ml or were undetectable at the set point (Fig. 1A). The former 18 animals are referred to as noncontrollers and the latter two as controllers in this study. Fifteen noncontrollers were euthanized with AIDS progression in 4 years (geometric mean survival period of 24 months), and the remaining three, after 1 or 2 years, are under observation (Table 2).

Group $A^+$ macaques, including two controllers, showed lower set point viral loads, whereas group $J^+$ macaques had higher viral loads (Fig. 1B). Viral loads in group $E^+$ and $B^+$ macaques were at intermediate levels. Multiple comparisons indicated significant

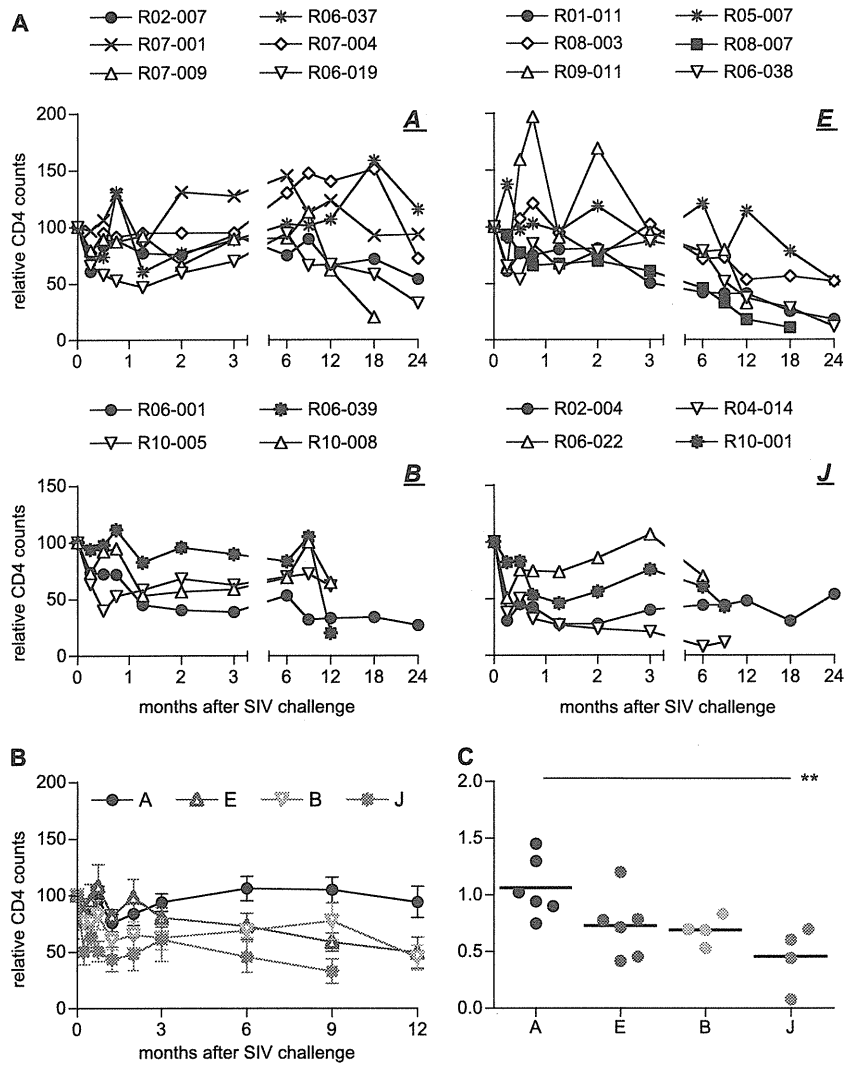


**FIG 2** Relative $CD4^+$ T-cell counts after SIVmac239 challenge. (A) Relative $CD4^+$ T-cell counts after challenge in $A^+$ (upper left), $E^+$ (upper right), $B^+$ (lower left), and $J^+$ (lower right) macaques. For each animal, the peripheral CD4 counts relative to that at challenge (set at 100) are shown. (B) Changes in means of relative $CD4^+$ T-cell counts after challenge in $A^+$ (black), $E^+$ (blue), $B^+$ (green), and $J^+$ (red) animals. (C) Comparison of relative $CD4^+$ T-cell counts at 6 months among four groups. Those in $J^+$ animals were significantly lower than those in $A^+$ ($P = 0.0090$ by one-way ANOVA and Tukey-Kramer's multiple-comparison test).

differences in set point plasma viral loads between groups $A^+$ and $J^+$ (Fig. 1C).

Most noncontrollers showed a decline in peripheral $CD4^+$ T-cell counts (Fig. 2A). Relative $CD4^+$ T-cell counts in the chronic phase were the highest in group $A^+$ animals and the lowest in group $J^+$ animals. Multiple-comparison tests revealed significant differences in relative $CD4^+$ T-cell counts at 6 months between groups $A^+$ and $J^+$ (Fig. 2B and C). Furthermore, multiple comparisons among groups $A^+$, $E^+$, and $J^+$ found significant differences in survival periods, which were the longest in $A^+$ and the shortest in $J^+$ animals (Table 2 and Fig. 3). These results indicate an association of MHC-I haplotypes with AIDS progression after SIV challenge in Burmese rhesus macaques.

**SIV antigen-specific $CD8^+$ T-cell responses.** We analyzed SIV-specific $CD8^+$ T-cell responses at 3 months and 1 year after SIV challenge by the detection of antigen-specific IFN-γ induction to examine which antigen-specific $CD8^+$ T-cell responses were induced predominantly (Table 3). Analysis revealed the predominant induction of Gag-specific and Nef-specific $CD8^+$ T-cell responses in group $A^+$ animals and Nef-specific $CD8^+$ T-cell responses in groups $E^+$ and $B^+$. Vif-specific $CD8^+$ T-cell responses were detected in three $J^+$ animals but not macaque R06-022, which rapidly developed AIDS in 5 months without detectable SIV-specific $CD8^+$ T-cell responses.

There was no significant difference in whole SIV antigen-specific $CD8^+$ T-cell responses among these four groups, although those responses were marginal or undetectable in two of four $J^+$ animals (Fig. 4A). However, Gag-specific $CD8^+$ T-cell frequencies at 3 months were significantly higher in $A^+$ animals (Fig. 4B). The analysis of four groups revealed inverse correlations between Gag-specific $CD8^+$ T-cell frequencies and plasma viral loads at 3 months ($P = 0.0087$; $r^2 = 0.3407$; data not shown). Three groups of $A^+$, $E^+$, and $B^+$ animals tended to show higher Nef-specific $CD8^+$ T-cell responses than $J^+$ animals (Fig. 4C).

**Viral genome mutations.** We then analyzed mutations in viral cDNAs amplified from plasma RNAs of group $A^+$, $E^+$, and $B^+$

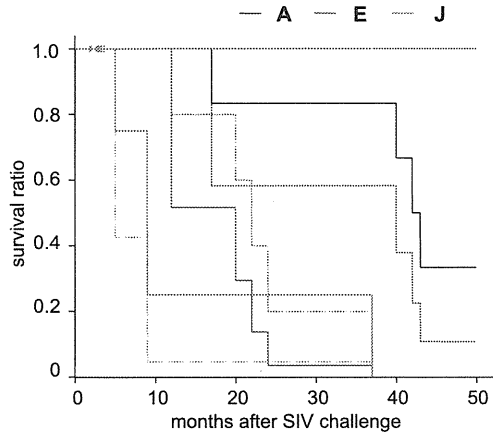


**FIG 3** Kaplan-Meyer survival curves after SIVmac239 challenge in $A^+$, $E^+$, and $J^+$ macaques. Macaque R08-003, which is under observation, is not included. $B^+$ animals were excluded from this analysis because data on only two animals were available. We determined the Kaplan-Meyer estimate of the survival function of each group and then compared the three curves using the log-rank test (Mantel-Cox test). Analysis showed significant differences in survival curves (chi square, 9.9; $P = 0.007$ by log-rank test of Kaplan-Meyer estimates).

macaques around 1 year after SIV challenge. Nonsynonymous mutations detected predominantly were as shown in Fig. 5. Multiple comparisons among groups $A^+$, $E^+$, and $B^+$ (Fig. 6) showed no differences in total numbers of nonsynonymous mutations but revealed significantly higher numbers of *gag* mutations in $A^+$ animals. $E^+$ animals had higher numbers of *tat* mutations than $A^+$ animals. There was no significant difference in the numbers of mutations in other regions, including *nef*, among these groups. Group $J^+$ animals were not included in the multiple comparisons, because three of them were euthanized by 9 months. These three had lower numbers of nonsynonymous mutations before their death, possibly reflecting lower immune pressure.

**Polyfunctionality in SIV-specific T-cell responses.** Finally, we investigated T-cell polyfunctionality to compare T-cell functions (2, 4, 45) in these four groups having different viral loads. We analyzed the polyfunctionality of SIV-specific $CD4^+$ and $CD8^+$ T cells around 8 months after challenge by the detection of SIV-specific induction of IFN-γ, TNF-α, IL-2, MIP-1β, and CD107a. SIV-specific $CD4^+$ T-cell polyfunctionality inversely correlated with plasma viral loads at around 9 months (Fig. 7A). We also found an inverse correlation between SIV-specific $CD8^+$ T-cell polyfunctionality and viral loads (Fig. 7A). However, there was no

**TABLE 3** SIV antigen-specific $CD8^+$ T-cell responses[a]

| MHC-I haplotype and time point after challenge | Macaque | $CD8^+$ T-cell response to: | | | | | | | | |
|---|---|---|---|---|---|---|---|---|---|---|
| | | Gag | Pol | Vif | Vpx | Vpr | Tat | Rev | Env | Nef |
| 3 mo | | | | | | | | | | |
| A | R02-007 | ND | ND | ND | ND | ND | ND | ND | ND | ND |
| A | R06-037 | 657 | — | 104 | — | — | — | — | — | 520 |
| A | R07-001 | 193 | — | — | — | — | — | — | — | 322 |
| A | R07-004 | 316 | — | 137 | — | — | — | — | — | 353 |
| A | R07-009 | 440 | — | 124 | — | — | — | — | 100 | 247 |
| A | R06-019 | 322 | — | — | — | — | — | — | — | 253 |
| E | R01-011 | — | — | 186 | — | — | — | — | — | — |
| E | R05-007 | — | — | — | — | — | 203 | — | — | 330 |
| E | R08-003 | — | — | — | — | — | — | — | — | 213 |
| E | R08-007 | — | — | — | — | — | — | — | 335 | — |
| E | R09-011 | — | — | 807 | — | 307 | — | — | 1,598 | 2,327 |
| E | R06-038 | 199 | — | 248 | — | — | 249 | — | 234 | 634 |
| B | R06-001 | — | 107 | 253 | 172 | — | — | — | 114 | 313 |
| B | R06-039 | — | — | — | — | — | — | — | 110 | 195 |
| B | R10-005 | 163 | 172 | — | 1,033 | 141 | — | 579 | — | 1,554 |
| B | R10-008 | — | — | — | 133 | — | — | 165 | — | — |
| J | R02-004 | — | — | 171 | — | — | 145 | — | 382 | 117 |
| J | R04-014 | — | 534 | 625 | 280 | 440 | 290 | 1,060 | — | 296 |
| J | R06-022 | — | — | — | — | — | — | — | — | — |
| J | R10-001 | — | — | 102 | — | — | — | — | — | — |
| 1 yr | | | | | | | | | | |
| A | R02-007 | — | — | 119 | — | — | — | — | 112 | 250 |
| A | R06-037 | 515 | — | 124 | 272 | 178 | — | — | — | 906 |
| A | R07-001 | 126 | — | — | — | — | — | — | — | 180 |
| A | R07-004 | — | — | — | — | — | — | — | — | 150 |
| A | R07-009 | 254 | 120 | 173 | — | 112 | — | — | 215 | 166 |
| A | R06-019 | 444 | 155 | 284 | — | 188 | — | — | 174 | 583 |
| E | R01-011 | 160 | — | — | — | — | — | — | — | 228 |
| E | R05-007 | — | — | — | — | — | — | — | — | — |
| E | R08-003 | — | — | — | — | — | — | — | — | 537 |
| E | R08-007 | — | — | — | — | — | — | — | — | 199 |
| E | R09-011 | — | 159 | — | — | — | — | 150 | 259 | 102 |
| E | R06-038 | 298 | 174 | 611 | — | — | 406 | 387 | 1,052 | 1,982 |
| B | R06-001 | — | — | — | — | — | — | — | 127 | 140 |
| B | R06-039 | — | — | — | — | — | 151 | — | — | — |
| B | R10-005 | 185 | — | — | — | — | — | — | — | — |
| B | R10-008 | 109 | 232 | — | — | — | — | 325 | — | 296 |
| J | R02-004 | 158 | — | — | — | — | — | — | — | — |
| J | R04-014[b] | 114 | 141 | 178 | — | — | 360 | 288 | — | 142 |
| J | R10-001[b] | — | — | — | — | — | — | — | — | — |

[a] Responses were measured by the detection of antigen-specific IFN-γ induction. Macaque R06-022, euthanized at 5 months, is not included in the lower portion. Antigen-specific $CD8^+$ T-cell frequencies (per 1 million PBMCs) are shown. ND, not determined; —, undetectable (<100).

[b] At 9 months (before euthanasia).

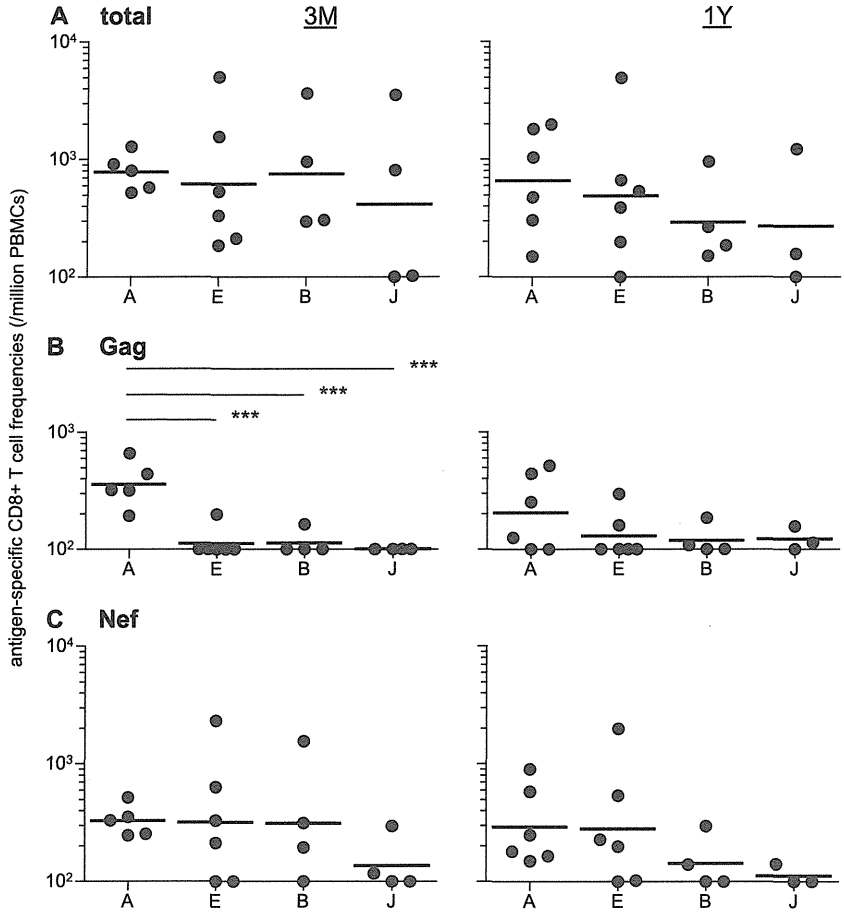


**FIG 4** Comparison of SIV antigen-specific $CD8^+$ T-cell responses. Responses were measured by the detection of antigen-specific IFN-γ induction using PBMCs at 3 months (3 M; left) and at 1 year (1Y; right). (A) Whole SIV antigen-specific $CD8^+$ T-cell frequencies. The sum of Gag-, Pol-, Vif-, Vpx-, Vpr-, Tat-, Rev-, Env-, and Nef-specific $CD8^+$ T-cell frequencies in each animal is shown. (B) Gag-specific $CD8^+$ T-cell frequencies. The frequencies at 3 months in $A^+$ animals were significantly higher ($A^+$ and $E^+$, $P < 0.0001$; $A^+$ and $B^+$, $P = 0.0003$; $A^+$ and $J^+$, $P < 0.0001$ by one-way ANOVA and Tukey-Kramer's multiple-comparison test). (C) Nef-specific $CD8^+$ T-cell frequencies.

correlation between viral loads and total SIV-specific $CD4^+$ T-cell or $CD8^+$ T-cell frequencies (Fig. 7B). Polyfunctional T-cell responses tended to be higher in group $A^+$ and lower in group $J^+$. Multiple comparisons revealed significant differences in SIV-specific $CD4^+$ T-cell polyfunctionality with the highest in group $A^+$ and the lowest in group $J^+$ (Fig. 7C). These results may reflect difference in disease progression among these animals.

## DISCUSSION

This study describes SIVmac239 infection in 20 Burmese rhesus macaques. Geometric means of set point plasma viral loads were approximately $10^5$ copies/ml. The levels are considered lower than those usually observed in the widely used SIVmac239 infection model of Indian rhesus macaques (28, 55) but are higher than those typically observed in untreated humans infected with HIV-1. While two $A^+$ animals controlled SIV replication, the remaining 18 Burmese rhesus macaques failed to control viremia. Indeed, all of the animals in the three groups $E^+$, $B^+$, and $J^+$ showed persistent viremia. Those noncontrollers, including four $A^+$ animals, developed AIDS in 0.5 to 4 years. These results indicate that the SIVmac239 infection of Burmese rhesus macaques does serve as an AIDS model.

In the present study, we compared SIVmac239 infections among four groups sharing MHC-I haplotypes A, E, B, and J, respectively. These animals showed differences in plasma viral loads, peripheral $CD4^+$ T-cell counts, survival periods, patterns of viral antigen-specific $CD8^+$ T-cell responses, polyfunctionality of SIV-specific T-cell responses, and numbers of viral genome mutations. These results indicate the association of MHC-I haplotypes with AIDS progression. There has been a number of reports describing SIV infections in macaques sharing a single or a couple of MHC-I alleles, but few studies have examined SIV infection in macaques sharing an MHC-I haplotype (10, 11, 40). SIV infection induces multiple epitope-specific $CD8^+$ T-cell responses, and $CD8^+$ T-cell responses specific for some MHC-I-restricted epitopes can be affected by those specific for other MHC-I-restricted epitopes due to CTL immunodominance (16, 29, 52). Thus, the preparation of macaque groups sharing MHC-I genotypes at the haplotype level, as described in the present study, would contribute to the precise analysis of SIV infection. The establishment of groups sharing both MHC-I haplotypes (56) may be ideal, but the accumulation of macaque groups sharing even one MHC-I haplotype could lead to the constitution of a more sophisticated primate AIDS model.

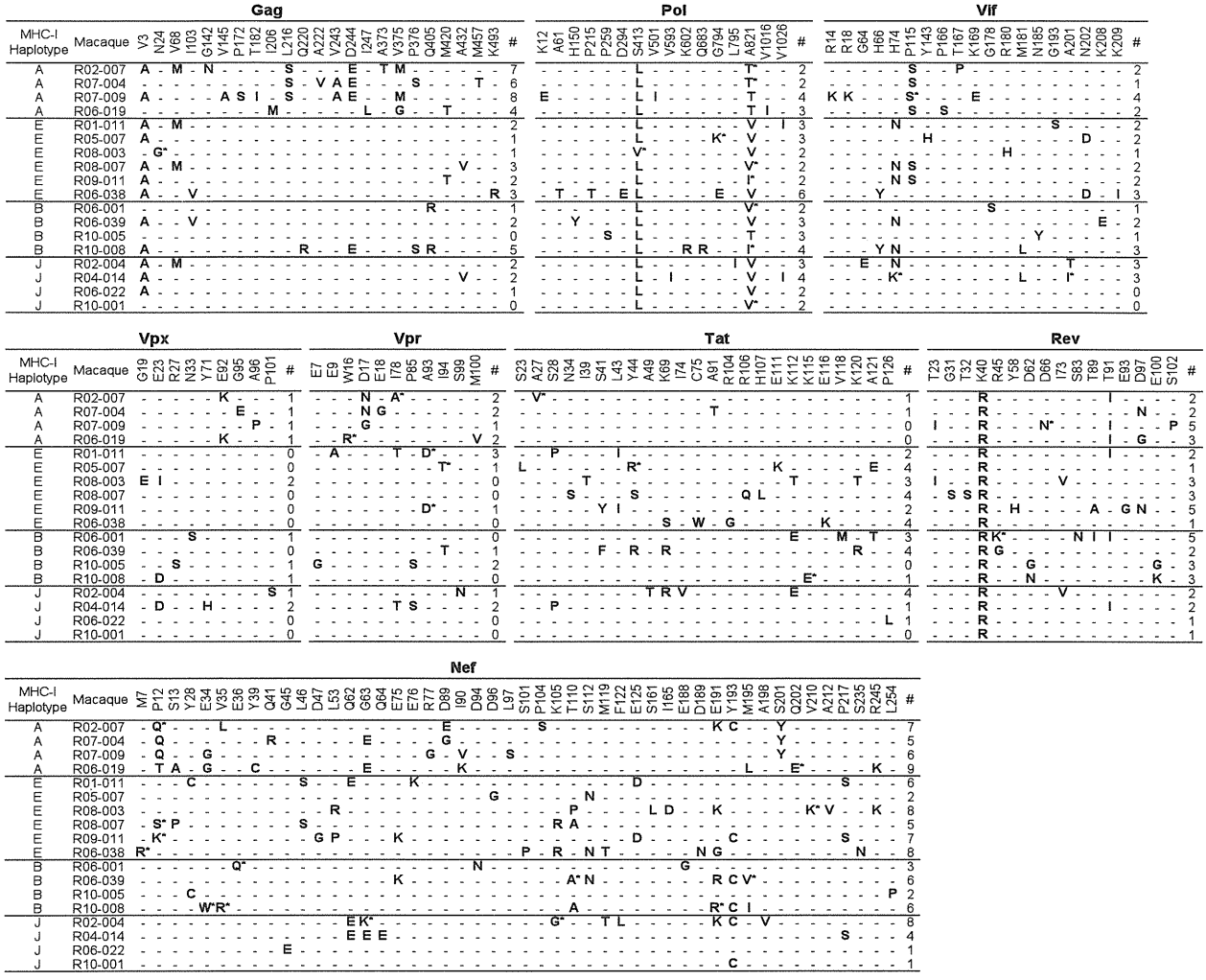


FIG 5 Predominant nonsynonymous mutations in viral cDNAs around 1 year after SIVmac239 challenge. Amino acid substitutions in SIV Gag, Pol, Vif, Vpx, Vpr, Tat, Rev, and Nef are shown. In three animals, R04-014, R06-022, and R10-001 in group $J^+$, data on the samples obtained before their death at 5 or 9 months after challenge are shown. Asterisks indicate the residues where different mutations were detected. It is known that amino acid substitutions at the Pol residues 413 and 821 and the Rev residue 40 are frequently observed in SIVmac239 infection and contribute to higher viral fitness *in vivo* (1, 39).

Various MHC-I alleles that do not consist of the first MHC-I haplotypes (A in $A^+$, E in $E^+$, B in $B^+$, and J in $J^+$ animals) were detected as shown in Table 4. Two $A^+$ macaques, R02-007 and R07-004, had two major alleles, *Mamu-A1*008:01* and *Mamu-B*007:02*, of MHC-I haplotype J, although their second MHC-I haplotype was not determined as J on the basis of information on the family tree. Even when these two animals were excluded from the $A^+$ group, multiple-comparison analyses showed significant

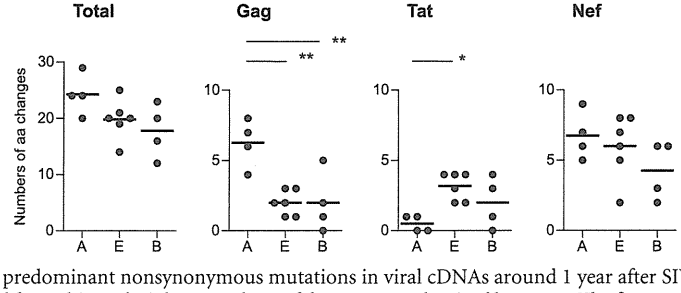


FIG 6 Comparison of the numbers of predominant nonsynonymous mutations in viral cDNAs around 1 year after SIVmac239 challenge among $A^+$, $E^+$, and $B^+$ macaques. $J^+$ animals were excluded from this analysis because three of them were euthanized by 1 year. The first graph (total) shows the sum of the numbers of amino acid substitutions in SIV Gag, Pol, Vif, Vpx, Vpr, Tat, Rev, and Nef. Gag, Tat, and Nef graphs show the numbers of Gag, Tat, and Nef amino acid substitutions, respectively. The numbers of Gag amino acid substitutions in $A^+$ animals were significantly higher than those in $E^+$ and $B^+$ animals ($A^+$ and $E^+$, $P = 0.0037$; $A^+$ and $B^+$, $P = 0.0069$ by one-way ANOVA and Tukey-Kramer's multiple-comparison test). The numbers of Tat amino acid substitutions in $E^+$ animals were significantly higher than those in $A^+$ animals ($P = 0.0140$).

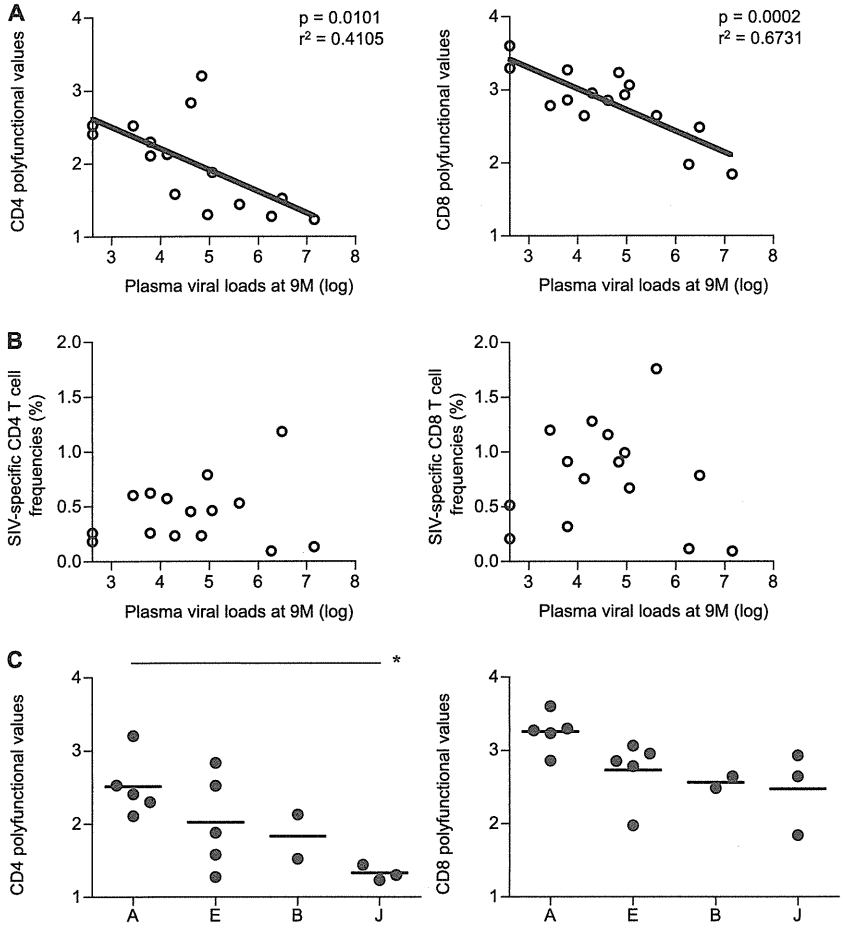


**FIG 7** Polyfunctionality in SIV-specific $CD4^+$ and $CD8^+$ T cells around 8 months after SIVmac239 challenge. Samples of macaques R02-007 ($A^+$), R01-011 ($E^+$), R10-005 ($B^+$), R10-008 ($B^+$), and R10-001 ($J^+$) were unavailable. (A) Correlation analysis of plasma viral loads at 9 months with polyfunctionality (polyfunctional values) of SIV-specific $CD4^+$ (left) and $CD8^+$ (right) T cells. Viral loads inversely correlated with SIV-specific $CD4^+$ ($P = 0.0101$; $r^2 = 0.4105$) and $CD8^+$ ($P = 0.0002$; $r^2 = 0.6731$) T-cell polyfunctionality. (B) Correlation analysis of plasma viral loads at 9 months with SIV-specific $CD4^+$ (left) and $CD8^+$ (right) T-cell frequencies (frequencies of $CD4^+$ and $CD8^+$ T cells showing the SIV-specific induction of induction of IFN-γ, TNF-α, IL-2, MIP-1β, or CD107a). (C) SIV-specific $CD4^+$ (left) and $CD8^+$ (right) T-cell polyfunctionality in $A^+$ ($n = 5$), $E^+$ ($n = 5$), $B^+$ ($n = 2$), and $J^+$ ($n = 3$) macaques. Multiple comparisons among $A^+$, $E^+$, and $J^+$ animals (excluding the $B^+$ group with available data on only two animals) revealed significant difference in SIV-specific $CD4^+$ T-cell polyfunctionality ($A^+$ and $J^+$, $P = 0.0195$ by one-way ANOVA and Tukey-Kramer's multiple-comparison test).

differences in plasma viral loads, peripheral $CD4^+$ T-cell counts, survival periods, Gag-specific $CD8^+$ T-cell responses, and numbers of viral gag mutations. These two $A^+$ animals were noncontrollers, supporting the notion that CTL responses specific for Mamu-A1*008:01- or Mamu-B*007:02-restricted epitopes are not efficient or effective. In addition, several MHC-I alleles were shared in two or three animals, but the influence of these alleles on disease progression remains unclear.

In the group $A^+$ animals that showed lower viral loads and slower disease progression, Gag-specific $CD8^+$ T-cell responses were efficiently induced, and their frequencies were significantly higher than those in the other three groups. Furthermore, these $A^+$ animals had higher numbers of nonsynonymous *gag* mutations, possibly reflecting strong selective pressure by Gag-specific $CD8^+$ T-cell responses. Previously, $CD8^+$ T-cell responses specific for the $Gag_{206\text{-}216}$ (IINEEAADWDL) epitope restricted by MHC-I haplotype A-derived Mamu-A1*043:01 and the $Gag_{241\text{-}249}$ (SSVDEQIQW) epitope restricted by A-derived Mamu-A1*065:01 have been shown to exert strong suppressive pressure on SIV replication (19, 21). In the present study, most $A^+$ animals selected escape mutations from these $CD8^+$ T-cell responses, GagL216S (a mutation leading to a leucine [L]-to-serine [S] substitution at the 216th amino acid in Gag) and GagD244E (aspartic acid [D]-to-glutamic acid [E] substitution at the 244th amino acid) or I247L (isoleucine [I]-to-L substitution at the 247th amino acid). These results are consistent with recent findings suggesting the potential of Gag-specific $CD8^+$ T-cell responses to efficiently suppress HIV-1/SIV replication (24).

In SIV-infected $A^+$ animals, predominantly Nef-specific as well as Gag-specific $CD8^+$ T-cell responses were elicited. At 3 months postchallenge, all of the $A^+$ animals showed relatively similar levels of total antigen-specific, Gag-specific, and Nef-specific $CD8^+$ T-cell responses, and their deviations appeared to be less than those in the other three groups. This may reflect the diminished influence of the second MHC-I haplotypes in these $A^+$ animals in the early phase of SIV infection, i.e., $CD8^+$ T-cell responses specific for epitopes restricted by MHC-I molecules derived from the second haplotypes may be suppressed by dominant $CD8^+$ T-cell responses specific for A-derived MHC-I-restricted epitopes.